

Reactions of Yttrium and Lanthanum Atoms with Nitrogen. Infrared Spectra of the Metal Nitrides and Dinitrogen Complexes in Solid Argon and Nitrogen

George V. Chertihin, William D. Bare, and Lester Andrews*

Department of Chemistry, University of Virginia, Charlottesville, Virginia 22901

Received: January 23, 1998; In Final Form: March 25, 1998

Laser-ablated Y and La atoms react with nitrogen to produce metal nitrides and dinitrogen complexes, whereas thermally evaporated Y and La atoms form only dinitrogen complexes. The ligated mononitride complexes $(\text{NN})_x\text{YN}$ and $(\text{NN})_x\text{LaN}$ at 771.6 and 761.7 cm^{-1} in solid nitrogen are identified from nitrogen-15 shifts. These complexes predict gas-phase fundamentals near 800 and 790 cm^{-1} respectively for YN and LaN. The $(\text{YN})_2$ and $(\text{LaN})_2$ molecules and dinitrogen complexes are also identified from nitrogen-15 shifts and result from the reaction of two metal atoms with a single dinitrogen molecule involving the $\text{Y}(\text{N}_2)$ and $\text{La}(\text{N}_2)$ intermediate species. The same saturated $(\text{YN})_2(\text{NN})_x$ and $(\text{LaN})_2(\text{NN})_x$ dinitrogen complexes are prepared on annealing solid argon containing 2% N_2 and deposition in pure nitrogen. The growth of ligated $(\text{YN})_2$ - $(\text{NN})_x$ and $(\text{LaN})_2(\text{NN})_x$ on annealing suggests that this nitrogen fixation reaction involves little activation energy.

Introduction

There are relatively few studies of second-row transition-metal atom reactions with dinitrogen: molybdenum and zirconium are the most thoroughly investigated,^{1–4} owing in part to the importance of molybdenum(III) complexes in dinitrogen cleavage.⁵ For the first member of the second series, YN, only a mass spectroscopic prediction of bond energies, all-electron ab initio calculations,⁶ and rotational analysis of the electronic spectrum⁷ have appeared.

Laser-ablated transition-metal atoms contain sufficient excess kinetic energy to dissociate molecular nitrogen and give rise to atom combination reactions to form mononitrides such as FeN .⁸ In condensation reactions of laser-ablated Sc atoms with argon-diluted N_2 , ScN , ScNN , and $(\text{ScN})_2$ were observed.⁹ It is noteworthy that $(\text{ScN})_2$, a rhombic ring with no N–N bond, was formed by the sequential reaction of two Sc atoms with a single N_2 molecule. Similar reactions of Ti, Zr, and Hf atoms with N_2 give evidence for analogous products and relativistic effects in the Hf species.¹⁰ In the present study, we report on matrix spectroscopic studies of reactions of Y and La atoms with N_2 and the observation of similar relativistic effects in Sc, Y, and La nitride series.

Experimental Section

The laser-ablation apparatus and techniques have been described previously.^{8,9} Rotating metal targets (Johnson-Matthey, 99.9%, lump) were ablated by 1064 nm laser radiation. Laser pulses (20–40 mJ) of 10 ns duration were focused onto $<10^{-2}$ cm^2 area, which gives on the order of 1 GW/cm^2 . Yttrium and lanthanum atoms were co-deposited with 2–4% N_2/Ar mixtures or pure N_2 samples ($^{14}\text{N}_2$, $^{15}\text{N}_2$, and mixtures) onto a 10 K CsI window. FTIR spectra were recorded on a Nicolet 750 spectrometer at 0.5 cm^{-1} resolution. Samples were annealed to allow diffusion and association of trapped species by turning off and restarting the refrigerator, to allow faster annealing, and more spectra were recorded at 10 K.

Thermal experiments were done by Klotzbucher at Mulheim using a resistively heated tantalum Knudsen cell and an

incorporated quartz crystal microbalance to control the metal sublimation rate as described previously.¹¹ Infrared spectra were recorded on a PE580 spectrophotometer at 2 cm^{-1} resolution and UV–vis spectra on a PE320 instrument, both coupled with a PE 3600 data station. Metal atoms (Y and La, Goodfellow, 99.9%) at relative matrix/metal atom ratios of better than 500/1 were co-deposited on a NaCl window maintained at 9 K along with either pure dinitrogen or N_2 diluted in argon.

Results

Below we present first the infrared spectra of Y and La atom reaction products with nitrogen diluted in argon, followed by the reactions with neat dinitrogen.

Y + N_2 Diluted in Ar. Infrared spectra are shown in Figure 1 for the laser-ablated Y + N_2 argon matrix system, and product absorptions are listed in Table 1. Sample deposition produced mainly bands at 2305, 1864.1/1856.6/1849.8, 1790.5, and 1767.9/1763.4 cm^{-1} in the high-frequency region and structured band systems starting at 710.4 and 586.9 cm^{-1} in the low-frequency region. In addition, weak YO and OYO absorptions¹² were detected at 842.9 and 617.8 cm^{-1} from target surface oxide contamination. Annealing produced strong bands at 2093.8, 2088.6, 1999.3, and 1809.5 cm^{-1} , a new 771.7 cm^{-1} band, and altered the 700 and 580 cm^{-1} band profile leading to strong new 677.4 and 558.9 cm^{-1} bands. Experiments with $^{15}\text{N}_2$ gave the same band profile and annealing behavior for the shifted band positions listed in Table 1 with the addition of a weak 775.7 cm^{-1} band that gave way on annealing to a new 749.4 cm^{-1} absorption. It is noteworthy that reaction with a $^{14}\text{N}_2$ + $^{15}\text{N}_2$ mixture gave all of the pure isotopic products in the lower frequency region (no intermediate components) and several new intermediate components (Table 1) in the upper frequency region.

Thermal Y atoms were condensed with 1% and 10% N_2 in argon, and the former reaction is illustrated in Figure 2 for the 2200–1700 cm^{-1} region. One immediately notes product absorptions, which are common to bands in the above laser-

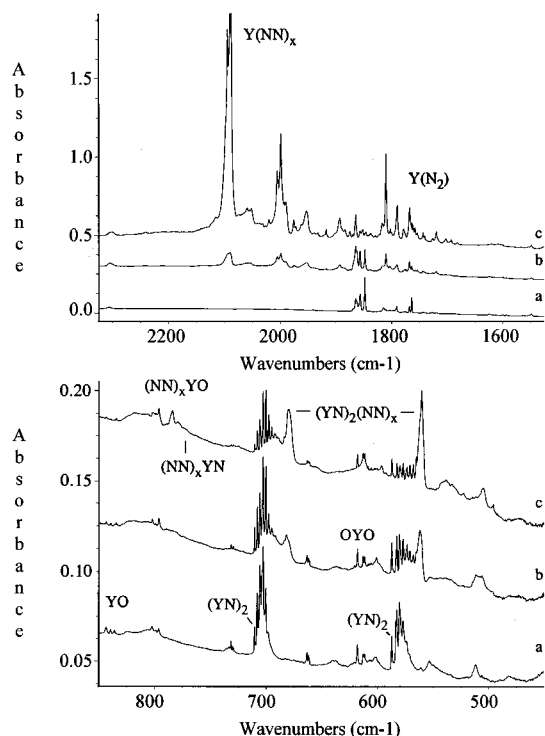


Figure 1. Infrared spectra in the 2325–1525 and 850–450 cm^{-1} regions for laser-ablated Y atoms deposited with 2% N_2 in argon: (a) sample deposited for 1 h at 10 K, (b) after annealing to 25 K, and (c) after annealing to 35 K. All spectra recorded at 10 K.

ablation experiments as is the annealing behavior of product absorptions. Here it is noteworthy in experiments with thermal yttrium atoms that no bands were observed at 2320, 771, 667, or 559 cm^{-1} . UV–visible spectra recorded on the same sample revealed the typical sharp “atomic yttrium” absorptions¹³ with strong features centered at 582, 440, 400, 387, 341, and 284 nm. Spectra recorded after annealing to 28 K, when the growth of new infrared absorptions in Figure 2c have appeared, indicate a loss in these bands by 40% and a new broad band growing in around 500 nm.

Y + N_2 . Figure 3 and Table 2 summarize the results of condensation of laser-ablated yttrium atoms with neat dinitrogen. The spectra are dominated by an extremely strong 2109 cm^{-1} band with structure and weaker bands at 2293.2, 1812.0, and 1758.4/1754.5 cm^{-1} . With thermal Y atoms, the sidebands on the strong 2109 cm^{-1} feature are better resolved, and the 1812 cm^{-1} feature appears as a doublet at 1812/1818 cm^{-1} with smaller satellites. Of particular interest in the laser ablation experiments are new bands at 3491.0, 2320.6, 771.6, 676.6, and 556.2 cm^{-1} , which were not observed in experiments with thermal atoms. These bands shifted with $^{15}\text{N}_2$ as given in Table 2. Experiments with a mixture of $^{14}\text{N}_2$ and $^{15}\text{N}_2$ gave pure isotopic doublets save for the latter two band systems where intermediate components were observed (Figure 3). An experiment with a statistical mixture ($^{14}\text{N}_2 + ^{14}\text{N}^{15}\text{N} + ^{15}\text{N}_2 = 1:2:1$) gave triplets for the 3491.0, 2320.6, 2293.2, 1758.4, 676.6, and 556.2 cm^{-1} band systems and a sharp 771.6 and 749.0 cm^{-1} doublet. Annealing pure nitrogen matrixes always produced a very strong green emission.

La + N_2 Diluted in Ar. Figure 4 and Table 3 present data for the $\text{La}/\text{N}_2/\text{Ar}$ reaction system. In the upper region, strong 1802.5 and 1770.7 cm^{-1} bands were observed on deposition; annealing decreased these bands in favor of a 1763.8 cm^{-1} satellite and increased a weak 2110 cm^{-1} band producing a strong 2113.9/2105.6 cm^{-1} doublet. Strong 652.3 and 529.9

TABLE 1: Absorptions (cm^{-1}) Observed in Reaction of Yttrium Atoms with Nitrogen on Condensation with Excess Argon

$^{14}\text{N}_2$	$^{15}\text{N}_2$	R (14/15)	anneal ^a	assignt
2319	2242	1.0343	+	$(\text{YN})_2(\text{NN})_x$
2305	2228	1.0345	+	$(\text{NN})_x\text{Y}(\text{N}_2)$
2093.8 ^b	2024.6	1.0341	+	$\text{Y}(\text{NN})_x$
2088.6 ^b	2019.6	1.0342	+	$\text{Y}(\text{NN})_x$
2055.6 ^b	1988.0	1.0340	+	$\text{Y}(\text{NN})_x$
1999.3 ^b	1933.0	1.0343	+, −	$\text{Y}(\text{NN})_x$
1953.5 ^b	1889.3	1.0340	+, −	$\text{Y}(\text{NN})_x$
1892.6 ^b	1830.2	1.0341	+, −	$\text{Y}(\text{NN})_x$
1864.1	1801.6	1.0347	+, −	YNN ?
1856.6	1794.7	1.0345	+, −	site
1849.8	1786.8	1.0353	+, −	site
1809.4	1749.4	1.0343	+	?
1790.5	1731.0	1.0344	+, −	$(\text{NN})_x\text{Y}(\text{N}_2)$
1767.9	1709.2	1.0343	+	$(\text{NN})_x\text{Y}(\text{N}_2)$
1763.4	1704.9	1.0343	−	$\text{Y}(\text{N}_2)$
1547.6 ^c	1498.4	1.0328	−	?
842.9	842.9	−	−	YO
801.8	801.8	1.0541	+	$(\text{NN})_x\text{YO}$
796.1	796.1	−	−	$(\text{NN})_x\text{YO}$
783.4	783.4	−	+	$(\text{NN})_x\text{YO}$
777.2	777.2	−	+	$(\text{NN})_x\text{YO}$
775.7	775.7	−	−	Y^{15}N
771.7	749.4	1.0298	+	$(\text{NN})_x\text{YN}$
731.5	710.4	1.0297	−	$(\text{YN})_2^+$ isolated (b_{2u})
729.6	708.6	1.0296	−	$(\text{YN})_2^+$ plus NN
710.4	689.9	1.0297	−	$(\text{YN})_2$ isolated (b_{2u})
708.0	687.6	1.0297	−	$(\text{YN})_2$ plus NN
705.7	685.4	1.0296	−	$(\text{YN})_2$ plus NN
702.8	682.6	1.0296	−	$(\text{YN})_2$ plus NN
700.4	680.2	1.0297	−	$(\text{YN})_2$ plus NN
698.0	677.9	1.0297	−	$(\text{YN})_2$ plus NN
695.3	675.3	1.0296	−	$(\text{YN})_2$ plus NN
677.4	657.9	1.0296	+	$(\text{YN})_2(\text{NN})_x$
617.8	617.8	−	−	saturated (b_{2u})
612.9	612.9	−	+	OYO
586.9	569.9	1.0298	−	$(\text{NN})_x\text{YO}_2$
582.4	565.5	1.0299	−	$(\text{YN})_2$ isolated (b_{3u})
580.1	563.1	1.0302	−	$(\text{YN})_2$ plus NN
576.9	560.2	1.0298	−	$(\text{YN})_2$ plus NN
573.3	556.6	1.0300	−	$(\text{YN})_2$ plus NN
570.7	554.2	1.0298	−	$(\text{YN})_2$ plus NN
567.8	557.4	1.0297	−	$(\text{YN})_2$ plus NN
558.9	542.9	1.0295	+	$(\text{YN})_2(\text{NN})_x$
511.2	495.3	1.0321	−	?
504.0	689.2	1.0303	+	?

^a Annealing behavior: + denotes increase, − denotes decrease.

^b New 2088.0, 2050.6, 2021.6, 1999.2, 1965.2, 1952.5, 1952.7, and 1893.1 cm^{-1} bands were observed with $^{14}\text{N}_2 + ^{15}\text{N}_2$. ^c The $^{14}\text{N}_2 + ^{15}\text{N}_2$ spectrum gave a triplet 1547.6, 1518.3, 1498.4 cm^{-1} .

cm^{-1} bands decreased on annealing in favor band sequences leading to broader bands at 635.5 and 512.5 cm^{-1} . Nitrogen-15 counterparts of these bands are listed in Table 3. Lanthanum oxide absorptions¹² were detected at 838.0, 796.8, 558.3, and 555.6 cm^{-1} . An experiment with a $^{14}\text{N}_2 + ^{15}\text{N}_2$ sample gave doublets for all bands; the lower region is illustrated in Figure 5, which shows the absence of intermediate mixed isotopic components.

Thermal La atoms co-condensed with 5% N_2 in argon produced a 2115 cm^{-1} band with a 2085 cm^{-1} shoulder; the 1802 cm^{-1} band appeared at 1812 cm^{-1} with a satellite at 1822 cm^{-1} . The 1770 cm^{-1} band was absent. Concurrent UV–vis spectra display features of “atomic lanthanum” on top of a broad band centered at 510 nm. They diminish upon annealing, while concurrently the 2115 cm^{-1} band appears in the infrared region.

La + N_2 . Laser-ablated La atoms collected at 10 K with

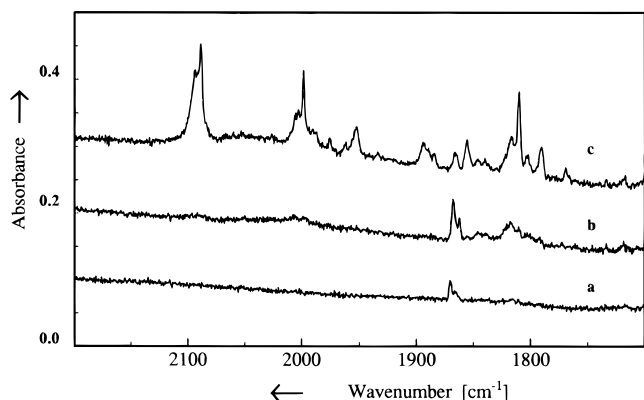


Figure 2. Infrared spectra in the 2200–1700 cm^{-1} region for thermally evaporated Y atoms deposited with 1% N_2 in argon at a concentration of 0.2% Y in argon: (a) sample deposited for 4.7 h at 9 K, (b) after annealing to 20 K, and (c) after annealing to 28 K. All spectra recorded at 9 K. Data from experiment by Klotzbucher.

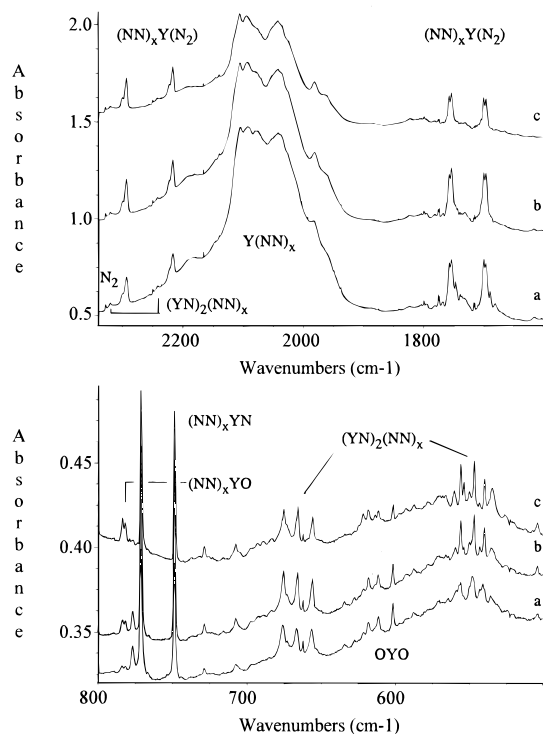


Figure 3. Infrared spectra in the 2340–1700 and 800–500 cm^{-1} regions for laser-ablated Y atoms deposited with pure nitrogen: (a) $^{14}\text{N}_2 + ^{15}\text{N}_2$ sample deposited for 2 h at 10 K, (b) after annealing to 25 K, and (c) after annealing to 35 K. All spectra recorded at 10 K.

pure nitrogen gave a very strong split band at 2136.2/2126.8/2111.7 cm^{-1} and weaker bands at 2320.6, 1810.2, and 1759.8 cm^{-1} in the upper region and strong 761.7, 633.3, and 512.2 cm^{-1} absorptions in the lower region. These bands shifted with pure $^{15}\text{N}_2$ as listed in Table 4. Figure 6 illustrates the spectrum in the lower region with a mixture of $^{14}\text{N}_2 + ^{15}\text{N}_2$: a strong doublet was observed at 761.7, 738.2 cm^{-1} , and the 633.6, 614.9 cm^{-1} and 512.2, 496.6 cm^{-1} doublets acquired weak 624.6 and 503.5 cm^{-1} intermediate components. Annealing to 25 K doubled the strong doublet and increased the 633.6, 614.9 cm^{-1} and 512.2, 496.6 cm^{-1} doublets by $A = 0.002$ and increased the 624.6 and 503.5 cm^{-1} intermediate components by $A = 0.004$ and produced a very strong green emission. Further annealing to 30 K (Figure 6c) increased the strong doublet another 25% (off scale) and left the above intermediate components stronger than the pure isotopic components. The

TABLE 2: Absorptions (cm^{-1}) Observed in Reaction of Yttrium Atoms with Nitrogen on Condensation with Excess Nitrogen

$^{14}\text{N}_2$	$^{15}\text{N}_2$	R (14/15)	anneal	assignt
2327.5	2249.8	1.0345	–	N_2
2320.6	2243.1	1.0346	+	$(\text{YN})_2(\text{NN})_x$
2302.4	2225.5	1.0346	+	$(\text{NN})_x\text{YN}$
2293.2 ^a	2216.5	1.0346	+	$(\text{NN})_x\text{Y}(\text{N}_2)$
2291.8	2214.8	1.0347	+	$(\text{NN})_x\text{Y}(\text{N}_2)$
2225.5	2180.4	1.0344	–	?
2109 ^b	2039	1.034	–	$\text{Y}(\text{NN})_x$
2079	2009	1.035	–	$\text{Y}(\text{NN})_x$
2050	1981	1.035	–	$\text{Y}(\text{NN})_x$
2026	1959	1.034	–	$\text{Y}(\text{NN})_x$
1812.0	1752.6	1.0339	+	site
1775.9 ^c	1716.9	1.0344	–	$(\text{NN})_x\text{Y}(\text{N}_2)$ site
3491.0 ^c	3376.3	1.0340	+	overtone
3482.8 ^c	3368.0	1.0341	+	overtone
1758.4 ^c	1700.2	1.0342	+	$(\text{NN})_x\text{Y}(\text{N}_2)$
1754.5 ^c	1696.0	1.0344	+	$(\text{NN})_x\text{Y}(\text{N}_2)$
1747.1	1689.0	1.0344	+	site
1738.7	1680.9	1.0344	+	site
1657.7	1603.3	1.0339	–	N_3
771.6	749.0	1.0302	+	$(\text{NN})_x\text{YN}$
728.9	707.6	1.0301	+	site
675.5 ^d	655.7	1.0302	+	$(\text{YN})_2(\text{NN})_x$ (b_{2u})
618.3	618.3			$(\text{NN})_x\text{YO}_2$
611.3	611.3			$(\text{NN})_x\text{YO}_2$
601.5	601.5			OYO
556.2	539.8	1.0304	+	$(\text{YN})_2(\text{NN})_x$ (b_{3u})

^a Doublet with $^{14}\text{N}_2 + ^{15}\text{N}_2$ and 2320, 2281, 2243 cm^{-1} and 2293/2256/2216 cm^{-1} triplet with $^{14}\text{N}_2 + ^{14}\text{N}^{15}\text{N} + ^{15}\text{N}_2$. ^b Broad unresolved band observed with both mixtures. ^c Doublets with $^{14}\text{N}_2 + ^{15}\text{N}_2$ and triplets 1775.9/1746.7/1716.9, 3491.0, 3482.8/3440.7, 3431.7/3376.3, 3368.0, 1758.4/1729.5/1700.4, and 1754.5/1725.6/1696.3 cm^{-1} with $^{14}\text{N}_2 + ^{14}\text{N}^{15}\text{N} + ^{15}\text{N}_2$. ^d Triplets 675.5/665.8/655.7 cm^{-1} and 556.2/546.9/539.8 cm^{-1} observed with both mixtures.

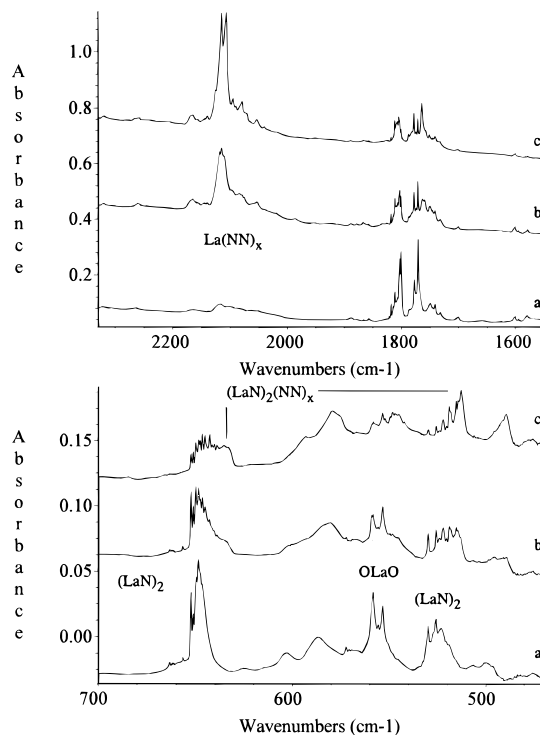


Figure 4. Infrared spectra in the 2340–1550 and 700–470 cm^{-1} regions for laser-ablated La atoms deposited with 2% N_2 in argon: (a) sample deposited for 1 h at 10 K, (b) after annealing to 25 K, and (c) after annealing to 35 K. All spectra recorded at 10 K.

spectrum in the upper region was the sum of pure isotopic components.

TABLE 3: Absorptions (cm^{-1}) Observed in Reaction of Lanthanum with Nitrogen on Condensation with Excess Argon

$^{14}\text{N}_2$	$^{15}\text{N}_2$	R (14/15)	anneal ^a	assignt
2318.7	2242	1.0342	+	$(\text{LaN})_2(\text{NN})_x$
2261.7	2187.5	1.0339	+, -	?
2113.9	2044.3	1.0340	+	$\text{La}(\text{NN})_x$
2105.6	2036.3	1.0340	+	site
2094.2	2027.8	1.0327	+	site
2078.4	2010.0	1.0340	+	$\text{La}(\text{NN})_x$
2053.4	1984.0	1.0350	+	$\text{La}(\text{NN})_x$
1889.3	1826.6	1.0343	+, -	LaNN ?
1802.5	1742.3	1.0346	-	$(\text{NN})_x\text{La}(\text{N}_2)$
1800.3	1740.3	1.0345	-	$(\text{NN})_x\text{La}(\text{N}_2)$
1777.6	1718.2	1.0345	-	$\text{La}(\text{N}_2)$
1770.7	1711.9	1.0345	-	$\text{La}(\text{N}_2)$
1763.8 ^b	1705.7	1.0341	+, +	$\text{La}(\text{N}_2)_2$
1749.7	1692.2	1.0340	-	site
1599.6	1548.0	1.0333	-	?
1578.1	1526.0	1.0341	-	$\text{La}(\mu\text{-N}_2)\text{La}$
838.0	838.0		-	LaO
652.3	632.6	1.0311	-	$(\text{LaN})_2$ isolated (b_{2u})
651.2	631.5	1.0312	-	$(\text{LaN})_2$ plus NN
649.9	630.3	1.0311	-	$(\text{LaN})_2$ plus NN
648.4	628.8	1.0312	-	$(\text{LaN})_2$ plus NN
647.5	628.0	1.0311	-	$(\text{LaN})_2$ plus NN
646.5	627.0	1.0311	-	$(\text{LaN})_2$ plus NN
645.1	625.8	1.0308	-	$(\text{LaN})_2$ plus NN
642.8	623.4	1.0311	-	$(\text{LaN})_2$ plus NN
640.4	621.2	1.0309	-	$(\text{LaN})_2$ plus NN
632.6	613.9	1.0305	+	$(\text{LaN})_2(\text{NN})_x$ saturated (b_{2u})
559	559		-	OLaO
529.9	513.5	1.0319	-	$(\text{LaN})_2$ isolated (b_{3u})
525.7	509.6	1.0316	-	$(\text{LaN})_2$ plus NN
524.2	508.2	1.0315	-	$(\text{LaN})_2$ plus NN
522.1	506.2	1.0314	-	$(\text{LaN})_2$ plus NN
520.4	504.6	1.0313	-	$(\text{LaN})_2$ plus NN
518.9	502.8	1.0324	-	$(\text{LaN})_2$ plus NN
515.4	499.7	1.0314	-	$(\text{LaN})_2$ plus NN
514.5	498.9	1.0313	-	$(\text{LaN})_2$ plus NN
512.5	496.9	1.0314	+	$(\text{LaN})_2(\text{NN})_x$ saturated (b_{3u})

^a Annealing behavior: + denotes increase, - denotes decrease.

^b Intermediate 1718.5 cm^{-1} band with $^{14}\text{N}_2 + ^{15}\text{N}_2$.

Finally, thermal La atoms condensed with nitrogen at 10 K gave the strong 2136 cm^{-1} band and weak 1810 and 1755 cm^{-1} bands with no 762 cm^{-1} absorption.

Sc + N₂. Infrared spectra of laser-ablated Sc atoms co-deposited with mixed isotopic nitrogen are illustrated in Figure 7 for comparison. Note two strong bands at 864.8 and 842.6 cm^{-1} with both mixtures that grow on annealing. In the statistical $^{14,15}\text{N}_2$ sample, very weak triplets at 739.2, 729.9, 720.3 and 641.2, 631.6, 624.8 cm^{-1} were detected on deposition and grew markedly on annealing. In the $^{14}\text{N}_2 + ^{15}\text{N}_2$ mixture, the initial spectrum for the deposited sample was dominated by the pure isotopic 739.2, 720.3 and 641.2, 624.8 cm^{-1} components, but annealing produced relatively more growth of the central, mixed isotopic components at 729.9 and 631.6 cm^{-1} .

Discussion

Taking into account recent results on similar transition metal-ligand systems,^{9,14} it is possible to identify the new product absorptions and to discuss reaction mechanisms. Thermal and laser-ablated Y and La atoms are compared for two reasons: (1) to understand the role of excess kinetic/electronic energy in laser-ablated relative to thermal atoms and (2) to reinforce the role of Y and La atoms in the primary reactions. The question always arises concerning the nature of the laser-ablated species.

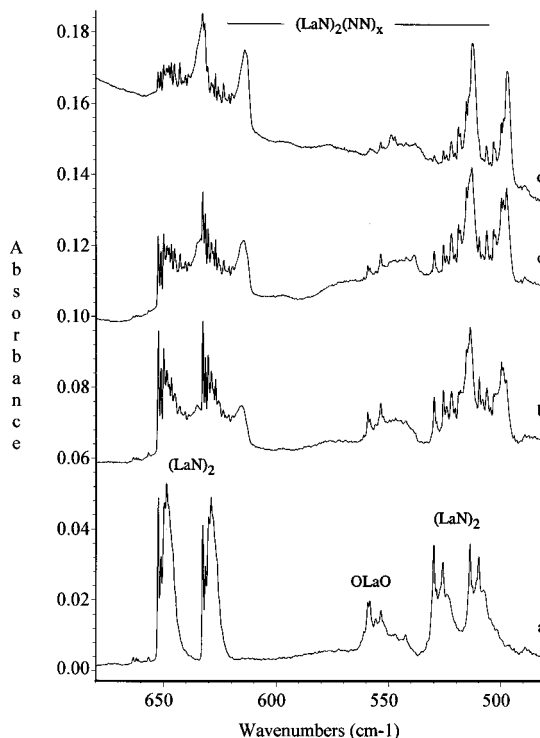


Figure 5. Infrared spectra in the 680–480 cm^{-1} region for laser-ablated La atoms deposited with 1% $^{14}\text{N}_2 + ^{15}\text{N}_2$ in argon: (a) sample deposited for 1 h at 10 K, (b) after annealing to 25 K, (c) after annealing to 30 K, and (d) after annealing to 40 K.

TABLE 4: Absorptions (cm^{-1}) Observed in Reactions of Lanthanum with Nitrogen on Condensation with Excess Nitrogen

$^{14}\text{N}_2$	$^{15}\text{N}_2$	R	anneal	assignt
2327.5	2249.8	1.0345	-	N_2
2320.6	2242.9	1.0346	+	$(\text{NN})_x\text{LaN}$
2317 sh	2240 sh	1.0343	+	$(\text{LaN})_2(\text{NN})_x$
2303.7	2226.9	1.0345	-	$(\text{NN})_x\text{LaN}$
2136.2	2065.5	1.0342	-	$\text{La}(\text{NN})_x$
2126.8	2057.6	1.0336	-	site
2111.7	2043.6	1.0333	-	site
2070.7	2002.6	1.0341	+, -	$\text{La}(\text{NN})_x$
2044.9	1977.4	1.0341	+, -	$\text{La}(\text{NN})_x$
2003.3	1937.5	1.0340	-	N_3^-
1810.2	1450.1	1.0343	+, -	$\text{La}(\text{N}_2)$
1808.9	1750.0	1.0337	+, -	$\text{La}(\text{N}_2)$ site
1761.9 ^a	1705.6	1.0342	-	$(\text{NN})_x\text{La}(\text{N}_2)$
1759.8 ^a	1701.6	1.0342	-	$(\text{NN})_x\text{La}(\text{N}_2)$
1657.7	1603.3	1.0339	-	N_3
777.8	753.6	1.0321	+	$(\text{NN})_x\text{LaN}$
775.7	751.7	1.0319	+	$(\text{NN})_x\text{LaN}$
761.7	738.2	1.0317	+	$(\text{NN})_x\text{LaN}$
689.8 ^b	668.7	1.0316	+	?
665.2	644.3	1.0316	+	?
641.2	627.7	1.0314	+	site
633.6 ^b	614.9	1.0312	+	$(\text{LaN})_2(\text{NN})_x$ (b_{2u})
596.0 ^b	679.3	1.0288	+	$(\text{LaNLaN})_x(\text{NN})_x$
515.0 ^b	499.2	1.0317	+, -	$(\text{LaN})_2(\text{NN})_x$ site
512.2 ^b	496.6	1.0314	+, -	$(\text{LaN})_2(\text{NN})_x$ (b_{3u})
510.7 ^b	495.1	1.0315	+, -	$(\text{LaN})_2(\text{NN})_x$ site
492.0 ^b	477.1	1.0312	+, -	site

^a A weak 1716.7 cm^{-1} intermediate component with $^{14}\text{N}_2 + ^{15}\text{N}_2$ may suggest coupling between end- and side-bound N_2 ligands.

^b Intermediate components 675.3, 624.6, 588.9, 506.7/503.5/502.1, and 486.8 cm^{-1} were observed with the $^{14}\text{N}_2 + ^{15}\text{N}_2$ mixture.

Kang and Beauchamp have shown, using an order of magnitude less laser power/ cm^2 than employed here, that laser-ablated Ni atoms have an average kinetic energy of 10 eV.¹⁵ Hence, the

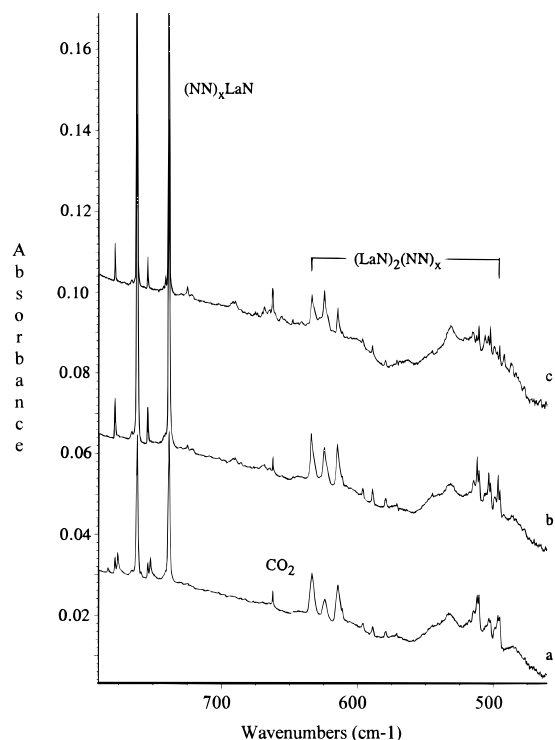


Figure 6. Infrared spectra in the 790–460 cm^{-1} region for laser-ablated La atoms deposited with pure nitrogen: (a) $^{14}\text{N}_2 + ^{15}\text{N}_2$ sample deposited for 2 h at 10 K, (b) after annealing to 25 K, and (c) after annealing to 30 K.

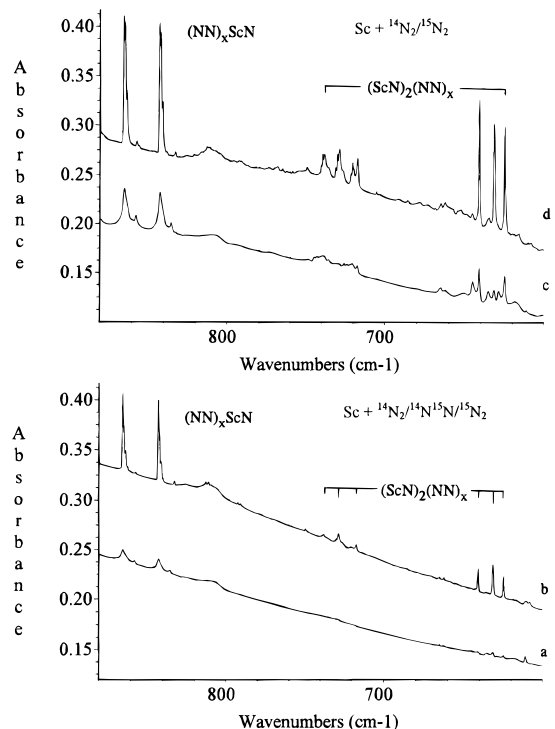


Figure 7. Infrared spectra in the 880–600 cm^{-1} region for laser-ablated Sc atoms deposited with mixed isotopic nitrogen: (a) $^{14}\text{N}_2/^{14}\text{N}^{15}\text{N}/^{15}\text{N}_2 = 1/2/1$ sample deposited for 1 h, (b) after annealing to 35 K, (c) $^{14}\text{N}_2/^{15}\text{N}_2 = 1/1$ sample deposited for 1.5 h, and (d) after annealing to 35 K.

present laser-ablated Y and La atoms are clearly hyperthermal and have an average kinetic energy in excess of 10 eV. Of course, some of this excess kinetic energy is absorbed by collisions with argon atoms before collision with N_2 . The role of laser-ablated metal cations and electrons in these experiments

is not known. It is presumed that neutralization of most species results before the matrix solidifies. In pure nitrogen matrixes N_3 radical and N_3^- absorptions are observed,^{8,16,17} but the latter is much weaker than the former. Clearly, the observation of N_3 radical attests to the formation of N atoms during the deposition process. Strong evidence that major reaction products contain a single metal atom requires the resolution of metal isotopic splittings, which are not possible for Y and La. However, similar experiments with Cr, Mo, and W have resolved metal isotopic splittings with natural isotopic abundance relative intensities,¹⁸ confirming that the major metal species in these reactions is monatomic.

Metal Mononitrides and Complexes. Strong bands were observed at 771.6 cm^{-1} for laser-ablated Y and at 761.7 cm^{-1} for laser-ablated La in pure nitrogen. These bands gave doublets with statistical and mixed isotopic nitrogen and 14/15 isotopic frequency ratios of 1.0302 and 1.0317, respectively, which are near the harmonic M–N diatomic values of 1.0301 and 1.0313. These bands were not observed with thermal Y and La atoms. In the case of Y and N_2 in argon, annealing produced a 771.7 cm^{-1} band, which gave a doublet with the nitrogen isotopic mixture and the ratio 1.0298 from the Y^{15}N component at 749.4 cm^{-1} . A sharp weak band at 775.7 cm^{-1} gave way on annealing to the 749.4 cm^{-1} band in the $^{15}\text{N}_2$ argon matrix experiment, but the ^{14}N counterpart of this 775.7 cm^{-1} band was masked by oxide impurity absorptions.

In similar Sc investigations, a sharp weak band at 913.0 cm^{-1} gave way on annealing to a broader 865.0 cm^{-1} band in solid argon, and a strong 864.8 cm^{-1} band and associated 2294.9 cm^{-1} absorption were observed in solid nitrogen.⁹ These bands exhibited diatomic Sc–N isotopic ratios and doublets with statistical mixed isotopes and were assigned to isolated ScN and the $(\text{NN})_x\text{ScN}$ complex, respectively, where x dinitrogen ligands are end-bonded to the metal center. The NN ligands apparently intensify the M–N vibrational mode. Similar effects have been observed for VN, CrN, and MnN in matrix isolation studies.¹⁴

By analogy with the scandium case, the strong analogous bands at 771.6 and 761.7 cm^{-1} are assigned to $(\text{NN})_x\text{YN}$ and $(\text{NN})_x\text{LaN}$, respectively, which are ligated metal nitrides. Weaker dinitrogen ligand stretching counterparts were observed at 2302.4 and 2303.7 cm^{-1} , respectively. How much perturbation does dinitrogen ligation have on these M–N fundamental vibrations? The shift is 48 cm^{-1} for ScN. The weak argon matrix band at 775.7 cm^{-1} is tentatively assigned to isolated Y^{15}N ; this predicts isolated Y^{14}N at 799.0 cm^{-1} , which was obscured in these experiments by $(\text{NN})_x\text{YO}$ absorption.¹² Accordingly, dinitrogen ligation results in a 27 cm^{-1} red shift for YN. (A similar 28 cm^{-1} red shift has been found for VN to $(\text{NN})_x\text{VN}$ in solid argon.¹⁴) A recent CASSCF calculation⁶ predicted a 807 cm^{-1} fundamental for the $1^1\Sigma^+$ ground state of YN, which is in excellent agreement with the above assignment. This assignment disagrees with a recent 661 cm^{-1} estimate of ω_e for YN from the Kratzer relationship using the 1.804 Å bond length.⁷ A similar discrepancy has been noted for ScN.⁹ Clearly, this correlation does not work for ScN and YN. The $(\text{NN})_x\text{LaN}$ complex suggests a LaN fundamental near 790 cm^{-1} . These bands represent the first vibrational observations and assignments of molecular YN and LaN species.

It should be pointed out that the YN and LaN fundamentals fall about 5% below the YO and LaO fundamentals.¹² A similar relationship was found for the ScO and ScN fundamental vibrations.⁹

With lanthanide metals, one wonders whether there is a

relativistic effect present, for example, in the bonding of LaN compared to YN. There appears to be a relativistic contraction of the LaN bond to compensate for the increase due to shell expansion which results in the frequency for the heavier LaN stretching fundamental being only slightly lower than the YN fundamental. This is best illustrated in the M–N stretching modes of the $(\text{NN})_x\text{ScN}$, $(\text{NN})_x\text{YN}$, and $(\text{NN})_x\text{LaN}$ complexes at 864.8, 771.6, and 761.7 cm^{-1} , respectively. A similar trend has been observed for $(\text{NN})_x\text{MN}$ complexes of Ti, Zr, and Hf at 940.6, 887.7, and 883.4 cm^{-1} , respectively.¹⁰ Relativistic effects are well-known for Hf in comparison to Zr.¹⁹

(MN)₂ Molecules. Recall that the reaction of laser-ablated Sc atoms with N₂ in argon gave sharp band systems at 772.2 and 672.9 cm^{-1} that increased first and then decreased on annealing in favor of strong bands at 2304.9, 735.9, and 641.3 cm^{-1} . The four lower bands exhibited 14/15 isotopic ratios for an Sc–N fundamental vibration whereas the upper band showed the ratio for a N–N mode. The former bands were assigned to the b_{2u} and b_{3u} antisymmetric stretching fundamentals of the rhombus-shaped $(\text{ScN})_2$ molecule in excellent agreement with DFT calculations, with no Sc–Sc or N–N bonding, and the latter bands to the $(\text{ScN})_2(\text{NN})_x$ complex, also produced in solid nitrogen,⁹ where the 2304.9 cm^{-1} band is due to a NN ligand mode and the 735.9 and 641.3 cm^{-1} bands are due to $(\text{ScN})_2$ in the ligated complex. This notation represents the $(\text{ScN})_2$ rhombic ring with extensive ligation of end-bound dinitrogen to both Sc positions and could as well be written as $(\text{NN})_x(\text{ScN})_2(\text{NN})_x$. Very similar behavior was observed for laser-ablated Y and La atoms, and analogous product bands will be assigned accordingly.

In the case of yttrium, sharp band systems beginning at 710.4 and 586.9 cm^{-1} in solid argon containing 2% N₂ gave way on annealing to 677.4 and 558.9 cm^{-1} bands, which exhibited 14/15 isotopic ratios just below the Y–N diatomic value, and a 2319 cm^{-1} band with dinitrogen isotopic behavior. The analogous nitrogen matrix experiments produced bands at 2320.6, 676.6, and 559.8 cm^{-1} . The latter bands gave triplet patterns with statistical ^{14,15}N₂ indicating the vibration of two equivalent nitrogen atoms in the metal nitride stretching region. Although the 2320.6 cm^{-1} band also showed a triplet pattern, this small perturbation from the N₂ fundamental at 2327.5 cm^{-1} denotes a weak interaction for the N₂ ligands and does not allow a definitive determination of the ligand orientation in this case.

The 710.4 and 586.9 cm^{-1} bands are assigned to b_{2u} and b_{3u} modes of the isolated rhombus-shaped $(\text{YN})_2$ molecule and the 2319–2320.6, 677.4–675.5, and 558.9–556.2 cm^{-1} bands to the saturated metal ligated species $(\text{YN})_2(\text{NN})_x$ in argon–nitrogen matrixes, with the upper bands due to the dinitrogen ligands. (Again, $(\text{NN})_x(\text{YN})_2(\text{NN})_x$ is implied here.) Now, let us consider the stepwise ligation of isolated $(\text{YN})_2$ to form the saturated ligand complex $(\text{NN})_x(\text{YN})_2(\text{NN})_x$. How many NN ligands are required? Six intermediate infrared bands are clearly resolved for each mode (Figure 1), and the spectrum suggests more unresolved absorption. It appears reasonable that at least four NN ligands can bond to each metal center, which would require more than seven intermediate bands as the isolated $(\text{YN})_2$ molecule ($x = 0$) is ligated by at least eight dinitrogen molecules to form the saturated complex. The sharp, weak 731.5, 729.6 cm^{-1} band system decreased on photolysis (not shown) and decreased on annealing in greater proportions than the 710.4 cm^{-1} band for isolated $(\text{YN})_2$. Density functional theory calculations (BP86/6-31+G*) predicted the b_{2u} fundamental of $(\text{ScN})_2^+$ to be 46 cm^{-1} above the neutral molecule value, and a similar band 35 cm^{-1} higher than $(\text{ScN})_2$ has been so

assigned.⁹ Likewise, the sharp 731.5, 729.6 cm^{-1} bands are probably due to $(\text{YN})_2^+$ formed by photoionization of $(\text{YN})_2$ by radiation from the laser plume in these experiments.

With lanthanum sharp band systems beginning at 652.3 and 529.9 cm^{-1} in solid argon behaved similarly and gave annealed counterparts at 2318.7, 633.6, and 512.3 cm^{-1} and nitrogen matrix counterparts at 2317, 633.5, and 512.5 cm^{-1} . The former bands are assigned to b_{2u} and b_{3u} modes of isolated $(\text{LaN})_2$ and the latter bands to the saturated $(\text{NN})_x(\text{LaN})_2(\text{NN})_x$ ligated species. Again, the spectrum for the stepwise $(\text{LaN})_2$ ligation process is similar to the $(\text{YN})_2$ case where eight intermediate bands are resolved (Figure 5) between isolated $(\text{LaN})_2$ and saturated $(\text{NN})_x(\text{LaN})_2(\text{NN})_x$ for the b_{2u} and b_{3u} modes of the rhombus chromophore.

MN₂ Molecules. Scandium deposited into pure nitrogen gave a strong 1699.4 cm^{-1} band, and Y and La follow in kind with 1758.4/1954.5 and 1759.8/1761.9 cm^{-1} bands, respectively. DFT calculations predicted ScNN and Sc(N₂) to have strong N–N stretching fundamentals at 1870 and 1744 cm^{-1} , and with appropriate isotopic behavior the 1699.4 cm^{-1} band was assigned to $(\text{NN})_x\text{Sc}(\text{N}_2)$.⁹ This species is considered side-bound Sc(N₂) with extensive ligation at Sc by end-bound dinitrogen. Analogous isotopic behavior and appropriate 14/15 isotopic frequency ratios for the 1758.4 and 1759.8 cm^{-1} bands leads to assignment to the side-bonded dinitrogen in the analogous $(\text{NN})_x\text{Y}(\text{N}_2)$ and $(\text{NN})_x\text{La}(\text{N}_2)$ ligated complexes, respectively. An experiment with Y and ¹⁴N₂/¹⁴N¹⁵N/¹⁵N₂ gave a triplet absorption pattern (Table 2) for two equivalent nitrogen atoms as required for the side-bound N₂ species. An overtone has been observed at 3368.5 cm^{-1} for the $(\text{NN})_x\text{Sc}(\text{N}_2)$ species⁹ and for several side-bonded lanthanide metal complexes²⁰ with fundamentals near 1750 cm^{-1} . The observation of a weak doublet at 3491.0/3482.8 cm^{-1} with 1.5% of the fundamental intensity and identical annealing behavior as the 1758.4/1754.5 cm^{-1} doublet ($A = 0.90$), with appropriate isotopic behavior in the weak 3376.3/3368.0 cm^{-1} doublet with 1.8% of the 1700.2/1696.0 cm^{-1} doublet intensity, verifies the overtone assignment. Note that twice the split fundamentals minus the split overtones gives $26.0 \pm 0.2 \text{ cm}^{-1}$ for the $(\text{Y}^{14}\text{N})_2$ species and $24.1 \pm 0.1 \text{ cm}^{-1}$ for the $(\text{Y}^{15}\text{N})_2$ species. Since overtones have been found for other side-bonded species, this supports the side-bonded assignment. Unfortunately, the $(\text{NN})_x\text{La}(\text{N}_2)$ fundamental ($A = 0.10$) was too weak for observation of the overtone.

The split 2293.2/2291.7 and 2216.5/2214.8 cm^{-1} ¹⁴N₂ and ¹⁵N₂ isotopic bands track with the 1758.4/1754.5 and 1700.2/1696.0 cm^{-1} isotopic bands, and the former are assigned to the strongest ligated end-bonded dinitrogen N–N stretching mode for $(\text{NN})_x\text{Y}(\text{N}_2)$. Similar bands at 2320.6 and 2242.9 cm^{-1} are assigned to ¹⁴N₂ and ¹⁵N₂ nitrogen isotopic terminal N–N ligand stretching modes in the analogous $(\text{NN})_2\text{La}(\text{N}_2)$ complex, respectively.

What is the nature of these $(\text{NN})_x\text{M}(\text{N}_2)$ complexes? The side-bonded $\text{M}(\text{N}_2)$ species in a pure nitrogen matrix will be subject to further ligation at the metal center, and we suggest, following the above examples of $(\text{NN})_x\text{MN}$ and $(\text{NN})_x(\text{MN})_2(\text{NN})_x$, that additional dinitrogen forms end-bound ligated complexes involving from one to at least four NN ligands.

In argon-diluted nitrogen matrix experiments, band systems were observed at 1864.1 and 1763.4 cm^{-1} for Y and at 1802.5 and 1770.7 cm^{-1} for La. The proximity of the 1763.4 and 1770.7 cm^{-1} bands to the above nitrogen matrix bands suggests assignment to isolated $\text{Y}(\text{N}_2)$ and $\text{La}(\text{N}_2)$. In the case of $\text{Y}(\text{N}_2)$, annealing reduces the 1763.4 cm^{-1} band in favor of 1767.9 and 1790.5 cm^{-1} bands, which are probably due to the beginnings

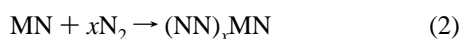
of stepwise ligation of end-bonded NN at the metal center. We have no conclusive assignment for the YNN and LaNN end-bonded species and speculate that these molecules rapidly add more dinitrogen in favor of the extensively ligated $(\text{NN})_x$ and $\text{La}(\text{NN})_x$ species. The 1864.1 cm^{-1} band is tentatively assigned to YNN, and a weak 1889.3 cm^{-1} band is in the region expected for LaNN in solid argon. The major product bands in each system for the coordinatively saturated metal center, noted $\text{M}(\text{NN})_x$, probably have $x = 6$, but we cannot determine x with confidence.

Reaction Mechanisms. The major difference between laser-ablated and thermally evaporated metal atoms is excess energy in the former,¹⁵ including metastable electronic energy shown to be important for manganese atoms²¹ and kinetic energy¹⁵ which has been shown to dissociate molecular nitrogen.^{8,14} With average kinetic energy of the ablated metal atoms in excess of 10 eV, a simple collision with N_2 can result in dissociation to N atoms.¹⁵ The observation of N_3 radical in nitrogen matrix experiments^{16,17} attests to the formation of N atoms in the laser-ablation investigations. Furthermore, the very strong green emission observed on annealing arises from recombination of N atoms.⁸

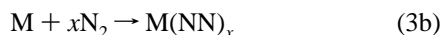
In the argon matrix experiments, YN is formed by direct combination of the atoms on the matrix surface produced in the laser-ablation process. In these experiments, the gas pressure between the target and cold window, less than 10^{-3} Torr, is sufficiently low to give a mean free path greater than the distance between target and cold window (2 cm).²¹ This suggests that most metal atoms collide with reagent molecules on the condensing surface layer.



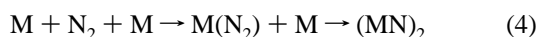
Unfortunately, we were not able to detect isolated LaN in the argon matrix studies. In the nitrogen matrix experiments both YN and LaN nitride products formed by atom combination are extensively ligated by end-bonded dinitrogen, which results in a small red shift in the Y–N and La–N vibrational fundamentals.



Thermal atoms, in fact cold atoms, react to form complexes (Figures 1 and 2), as the products of reactions 3 increase on annealing.

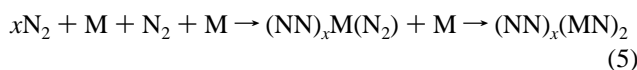


The $(\text{ScN})_2$, $(\text{YN})_2$, and $(\text{LaN})_2$ species are formed without intermediate $^{14}\text{N}^{15}\text{N}$ isotopic components from mixed $^{14}\text{N}_2 + ^{15}\text{N}_2$ samples, which means that a single dinitrogen molecule is reduced to $(\text{MN})_2$ by two metal atoms probably involving a MN_2 intermediate. This dissociation of molecular nitrogen by two bare transition-metal atoms is, in effect, a nitrogen fixation reaction.



The first reaction of metal atoms with N_2 , reaction 3a, proceeds spontaneously, as demonstrated by the increase of infrared product absorptions on annealing cold samples (Figures 1 and 2). This annealing operation is accompanied by the decrease of ultraviolet–visible atomic absorption attesting to

the spontaneous reaction of metal atoms to form dinitrogen complexes, the intermediate species in reaction 4, which increase on annealing. Although reaction 4 may proceed on annealing in solid argon without appreciable activation energy, the growth of $(\text{MN})_2$ is in the ligated $(\text{NN})_x(\text{MN})_2(\text{NN})_x$ complexes. However, in solid nitrogen, there is a clear growth of the $(\text{NN})_x\text{M}(\text{N}_2)$ and $(\text{NN})_x(\text{MN})_2(\text{NN})_x$ species on annealing, reaction 5, which proceeds through the $(\text{NN})_x\text{M}(\text{N}_2)$ intermediate without activation energy.



Conclusions

Laser-ablated Y and La atoms react with nitrogen to produce metal nitrides and dinitrogen complexes, whereas thermally evaporated Y and La atoms form only the dinitrogen complexes. The mononitride complexes $(\text{NN})_x\text{YN}$ and $(\text{NN})_x\text{LaN}$ at 771.6 and 761.7 cm^{-1} in solid nitrogen are identified from nitrogen-15 shifts and involve end-bound NN ligands on the metal centers. Gas-phase fundamentals for YN and LaN can be predicted near 800 and 790 cm^{-1} , respectively, from these complexes. The isolated $(\text{YN})_2$ and $(\text{LaN})_2$ molecules in solid argon are also identified from nitrogen-15 shifts and result from the reaction of two metal atoms with a single dinitrogen reagent molecule, and the saturated $(\text{NN})_x(\text{YN})_2(\text{NN})_x$ and $(\text{NN})_x(\text{LaN})_2(\text{NN})_x$ complexes produced on annealing solid argon containing 2–4% N_2 to allow stepwise ligation of NN at both metal centers have nearly the same frequencies as those formed in pure nitrogen. These experiments have shown that two Y or two La atoms can reduce molecular nitrogen to a dimetal dinitride, an open rhombic ring, which is a nitrogen fixation reaction.

Acknowledgment. We are indebted to W. E. Klotzbucher for the personal communication of preliminary thermal Y and La experimental results and for allowing us to report and compare his thermal metal atom with our laser-ablated metal atom results.

References and Notes

- (1) Bates, J. K.; Dunn, T. M. *Can. J. Phys.* **1976**, *54*, 1216.
- (2) Bates, J. K.; Gruen, D. M. *J. Mol. Spectrosc.* **1979**, *78*, 284.
- (3) Fletcher, D. A.; Jung, J. A.; Steimle, T. C. *J. Chem. Phys.* **1993**, *99*, 901. Lian, L.; Mitchell, S. A.; Rayner, D. M. *J. Phys. Chem.* **1994**, *98*, 11637.
- (4) Sze, N. S.-K.; Cheung, A. S.-C. *J. Quant. Spectrosc. Radiat. Transfer* **1994**, *52*, 145; *J. Mol. Spectrosc.* **1995**, *174*, 194 and references therein.
- (5) Cohen, J. D.; Mylvaganam, M.; Fryzuk, M. D.; Loehr, T. M. *J. Am. Chem. Soc.* **1994**, *116*, 9329. Laplaza, C. E.; Johnson, M. J. A.; Peters, J. C.; Odom, A. L.; Kim, E.; Cummins, C. C.; George, G. N.; Pickering, I. *J. J. Am. Chem. Soc.* **1996**, *118*, 8623 and references therein.
- (6) Gingrich, R. A. *J. Chem. Phys.* **1968**, *49*, 19. Shim, I.; Gingerich, K. A. *Int. J. Quantum Chem.* **1993**, *46*, 145.
- (7) Ram, R. S.; Bernath, P. F. *J. Mol. Spectrosc.* **1994**, *165*, 97.
- (8) Chertihin, G. V.; Andrews, L.; Neurock, M. *J. Phys. Chem.* **1996**, *100*, 14609.
- (9) Chertihin, G. V.; Andrews, L.; Bauschlicher, C. W., Jr. *J. Am. Chem. Soc.* **1998**, *120*, 3205.
- (10) Kushto, G. P.; Souter, P. F.; Chertihin, G. V.; Andrews, L., to be published.
- (11) Klotzbücher, W. E.; Petrukhina, M. A.; Sergeev, G. B. *J. Phys. Chem. A* **1997**, *101*, 4548.
- (12) Chertihin, G. V.; Bare, W. D.; Andrews, L., to be published (Y and La oxides).
- (13) Martin, W. C.; Zlaubas, R.; Hagen, L. *Atomic Energy Levels—The Rare Earth Elements*; Natl. Stand. Ref. Data Sys.; National Bureau of Standards: Washington, DC, 1978.
- (14) Andrews, L.; Bare, W. D.; Chertihin, G. C. *J. Phys. Chem. A* **1997**, *101*, 8417.

- (15) Kang, H.; Beauchamp, J. L. *J. Phys. Chem.* **1985**, *89*, 3364.
(16) Tian, R.; Facelli, J. C.; Michl, J. *J. Phys. Chem.* **1988**, *92*, 4073.
(17) Hassanzadeh, P.; Andrews, L. *J. Phys. Chem.* **1992**, *96*, 9177.
(18) Chertihin, G. V.; Bare, W. D.; Andrews, L. *J. Chem. Phys.* **1997**, *107*, 2798 and unpublished results.
(19) Pyykkö, P. *Chem. Rev.* **1988**, *88*, 563.
(20) Willson, S. P.; Andrews, L., to be published.
(21) Chertihin, G. V.; Andrews, L. *J. Phys. Chem. A* **1997**, *101*, 8547.